Thermoanalytical investigations of tris(ethylenediamine)nickel(II) oxalate and sulphate complexes

TG–MS and TR–XRD studies

K. S. Rejitha · Suresh Mathew

Abstract Investigations on the thermal behaviour of $[Ni(en)_3]C_2O_4 \cdot 2H_2O$ and $[Ni(en)_3]SO_4$ have been carried out in air and helium atmosphere. Simultaneous TG/DTA coupled online with mass spectroscopy (MS) in helium atmosphere detected the presence of H_2, O, CO, N_2/$CH_2=CH_2$ and CO_2 fragments during the decomposition of tris(ethylenediamine)nickel(II) oxalate and H_2, O, NH, NH_2, NH_3 and N_2/$CH_2=CH_2$ fragments for tris(ethylenediamine)nickel(II) sulphate complex. The thermal events during the decomposition were monitored by temperature-resolved X-ray diffraction. In air, both the complexes give nickel oxide as the final product of the decomposition. In helium atmosphere, tris(ethylenediamine)nickel(II) oxalate gives nickel as the residue, whereas tris(ethylenediamine)nickel(II) sulphate gives a mixture of nickel and nickel sulphide phases as the final residue. Kinetic analyses of these complexes by isoconversional methods are discussed and compared.

Keywords Mass spectroscopy · Temperature resolved X-ray diffraction · Kinetic analysis · Isoconversional method

Introduction

Amines like propylenediamine, ethylenediamine and ammonia are well known for their complexing capacity and they form well-defined complexes with transition metals.

K. S. Rejitha · S. Mathew (✉)
School of Chemical Sciences, Mahatma Gandhi University, P.D. Hills P.O., Kottayam, Kerala 686-560, India
e-mail: sureshmathews@sancharnet.in

During heating these complexes undergo stepwise decomposition to form various intermediates [1, 2]. Among these ethylenediamine complexes are well studied and these complexes are thermally stable due to the chelating effect [3]. It is well known that experimental conditions have a telling effect on the thermal decomposition pattern of the complexes. In air, most of the complexes give metal oxide as the final residue [3]. However, in inert condition metal is obtained as the final product [2]. In this study, we have investigated in detail the thermal decomposition of two nickel complexes containing ethylenediamine as the ligand viz., tris(ethylenediamine)nickel(II) oxalate dihydrate and tris(ethylenediamine)nickel(II) sulphate in dynamic air and helium. We have detected the evolved gaseous species and studied the structural changes happening during the decomposition of amine complexes by TG–MS and temperature-resolved XRD. Despite numerous reports in the literature with regard to the thermal decomposition studies on the nickel amine complexes, the aforesaid aspects have not been much investigated yet [2].

We have also studied the thermal decomposition kinetics of tris(ethylenediamine)nickel(II) oxalate dihydrate and tris(ethylenediamine)nickel(II) sulphate using model-free isoconversional methods viz., Flynn–Wall–Ozawa (FWO) [4, 5], Friedman [6] and Kissinger–Akahira–Sunose (KAS) [7, 8].

Experimental

The complexes were synthesized employing reported procedures [9, 10]. Nickel content in the complexes was determined by means of gravimetry [11]. The complexes were further characterized by spectral and chemical analysis.

Instrumentation

Thermogravimetric analyses in air were carried out using Shimadzu DTG-60 instrument connected to a TA-60 online analyser. The heating rates employed were 5, 10, 15 and 20 °C min^{-1}. TG–MS studies were carried out using a Rigaku, TG-8120 thermogravimetric apparatus combined with mass spectroscopy (Anelva, M-QA200TS) at a heating rate of 10 °C min^{-1} under high-purity He gas flow (99.9999%). For the thermogravimetric analyses, the sample mass used were 10 ± 0.2 mg for all the experiments.

The elemental analyses were carried out using Vario Elemental III instrument. X-ray powder patterns were recorded on a Bruker D8 Advance diffractometer using Cu Kα radiation, $\lambda = 1.542$ Å attached with a programmable temperature device from Anton Paar, (TTK 450). The measurements were performed by placing the sample on a flat sample holder, while the samples were heated by the programmable temperature controller. A series of diffraction patterns were recorded at every 20 °C rise of temperature. Crystallite size was calculated using Scherrer equation

$$t = 0.9\lambda/\beta\cos\theta,$$

where t is the thickness of the particle, λ is the wave length, β is full width at half maximum (FWHM) intensity (in radians) and $\cos\theta$ is the corresponding angle. Morphology of the complexes, intermediates formed at different temperatures and the residues were determined using JEOL JSM-6390 scanning electron microscope. For SEM analyses, the samples were spread on a carbon tape and made uniform by blowing air.

Kinetic studies

Isoconversional methods

Solid state reaction often follows the basic kinetic equation:

$$\frac{d(\alpha)}{dt} = A \exp\frac{-E}{RT}f(\alpha), \tag{1}$$

where A is the pre-exponential factor, E is the activation energy, R is the gas constant, T is the temperature and $f(\alpha)$ is the kinetic model function. For a nonisothermal reaction, Eq. 1 can be written as:

$$\frac{d(\alpha)}{f(\alpha)} = \frac{A}{\phi}\exp\frac{-E}{RT}dT, \text{ where the heating rate } \phi = \frac{dT}{dt}. \tag{2}$$

The above equation pertains to a single step reaction kinetics, but quite often the solid state reactions contain complex reaction steps and a single rate equation is unable to explain the complexities of solid state reactions. In this context, isoconversional methods could be used as an alternative to study the solid state reactions. Now a days model-free isoconversional methods have gained much attention as a useful approach to investigate the kinetics of the solid state reactions as these methods possess several advantages over conventional approaches [12–15]. These methods are based on the principle that the reaction rate at a constant extent of conversion (α) is only a function of the temperature (T). For a single step reaction, the activation energy (E) is constant over the whole conversion function. For multi step kinetics, the activation energy (E) vary with the extent of conversion and this reflects the variation in relative contributions of single steps to the overall reaction rate. Friedman, FWO and KAS are isoconversional methods and are frequently employed to study the kinetics. These methods yield effective activation energy (E) as a function of extent of conversion (α) [16].

In order to study the kinetics using the model-free methods, several TG measurements were carried out at different heating rates. Friedman, Flynn–Wall–Ozawa (FWO) as well as KAS methods are based on multiple heating rate experiments.

Flynn–Wall–Ozawa equation is as follows [4, 5]:

$$\ln\phi = \ln\frac{AE}{R} - \ln g(\alpha) - 5.3305 - 1.052\frac{E}{RT}, \tag{3}$$

where ϕ is the heating rate, α is the degree of conversion, $g(\alpha)$ is the mechanism function, E is the activation energy, A is the pre-exponential factor and R is the gas constant.

Friedman equation is [6]:

$$\ln\frac{d\alpha}{dt} = \ln[Af(\alpha)] - \frac{E}{RT}, \tag{4}$$

where $\frac{d\alpha}{dt}$ is the rate of conversion and $f(\alpha)$ is the mechanism function.

Kissinger–Akahira–Sunose (KAS) equation is [7, 8]:

$$\ln\left(\frac{\phi}{T^2}\right) = \ln\frac{AR}{Eg(\alpha)} - \frac{E}{RT}. \tag{5}$$

From the above equations (3–5), plots of $\ln\phi$ versus $1/T$, $\ln\frac{d\alpha}{dt}$ versus $1/T$, $\ln\frac{\phi}{T^2}$ versus $1/T$ give straight lines with slopes $-1.052E/R$, $-E/R$ and $-E/R$, respectively, for the FWO, Friedman and KAS equations. The slope of the straight line is directly proportional to the activation energy.

Results and discussion

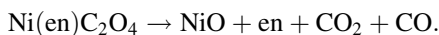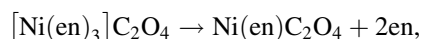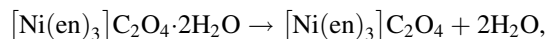### Thermal decomposition studies

Tris(ethylenediamine)nickel(II) oxalate dihydrate

The details of the elemental analyses are given in Table 1, which are in agreement with the formulae of the

Table 1 Elemental analysis/%

Complexes	Ni Obsd./calc.	C Obsd./calc.	H Obsd./calc.	N Obsd./calc.	S
$[Ni(en)_3]C_2O_4 \cdot 2H_2O$	16.2/15.9	26.5/26.6	7.7/7.2	25.1/24.9	
$[Ni(en)_3]SO_4$	17.5/17.5	21.5/21.5	7.2/7.2	25.1/25	9.6/9.6

complexes. For tris(ethylenediamine)nickel(II) oxalate dihydrate, the decomposition in air involves three stages. The decomposition pattern of the complex in air is as follows:

$$[Ni(en)_3]C_2O_4 \cdot 2H_2O \rightarrow [Ni(en)_3]C_2O_4 + 2H_2O,$$

$$[Ni(en)_3]C_2O_4 \rightarrow Ni(en)C_2O_4 + 2en,$$

$$Ni(en)C_2O_4 \rightarrow NiO + en + CO_2 + CO.$$

TG/DTA plot for the thermal decomposition of the complex in air at a heating rate of 10 °C min^{-1} is shown in Fig. 1. The values of the temperature of inception (T_i), final temperature (T_f) and the temperature of summit (T_s) for the thermal decomposition and the mass loss data are given in Table 2. From the TG curve, it is seen that the complex starts to lose mass at 70 °C. The first stage in the thermogram corresponds to the loss of two molecules of water in the temperature range 70–135 °C. This dehydration resulted
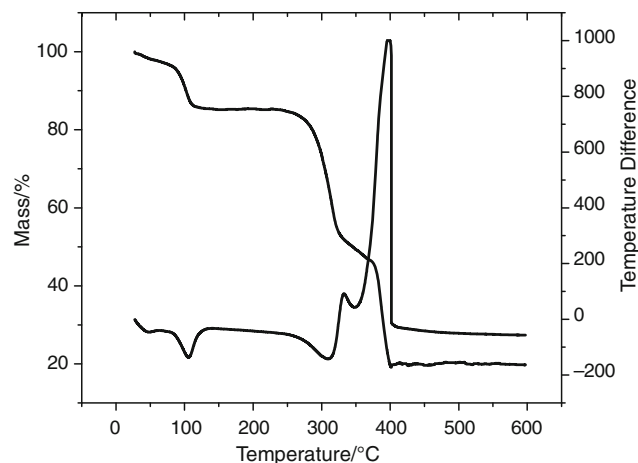
Fig. 1 TG/DTA plot of tris(ethylenediamine)nickel(II) oxalate dihydrate (in air) at heating rate 10 °C min^{-1}

in a stable complex i.e. tris(ethylenediamine)nickel(II) oxalate. The second stage commences at 260 °C and corresponds to the loss of two molecules of ethylenediamine to give mono(ethylenediamine)nickel(II) oxalate. This monoamine intermediate is not stable and quickly decomposes at 325 °C. The final stage corresponds to the decomposition of this monoamine intermediate by the loss of one molecule of ethylenediamine along with the evolution of CO and CO$_2$ to form NiO as the residue. The DTA results complement this observation. The DTA pattern contains two endotherms at 105 and 312 °C and one exotherm at 395 °C. The two endotherms correspond to the dehydration and the deamination reactions while the exotherm corresponds to the decomposition of mono(ethylenediamine)nickel(II) oxalate to give NiO in an oxidizing atmosphere. A shoulder of an exothermic peak at 332 °C is seen in the DTA curve. This can be due to the overlapping of two reactions viz., the deamination and the decomposition reactions in the final stage. Under oxidizing condition ethylenediamine is oxidized instantaneously to oxides of nitrogen and carbon and the exotherm at 395 °C in the DTA can be attributed to the oxidation of ethylenediamine. The obtained results are in agreement with the reported thermal decomposition pattern of the complex [9].

The plot of simultaneous TG/DTA coupled online with MS spectra carried out under helium atmosphere is shown in Fig. 2. In helium atmosphere, the dehydrated (dehydration occurs due to the heating of the sample before MS analysis) tris(ethylenediamine)nickel(II) oxalate complex undergoes a two step decomposition pattern as shown below:

$$[Ni(en)_3]C_2O_4 \rightarrow NienC_2O_4 + 2en,$$

$$NienC_2O_4 \rightarrow Ni + en + CO_2 + CO + O.$$
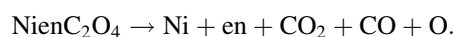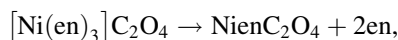
The deamination stage occurs at 245 °C in helium (inert) atmosphere with the liberation of two ethylenediamine

Table 2 Phenomenological data for the thermal decomposition of tris(ethylenediamine)nickel(II) oxalate dihydrate in air/$\phi = 10$ °C min^{-1}
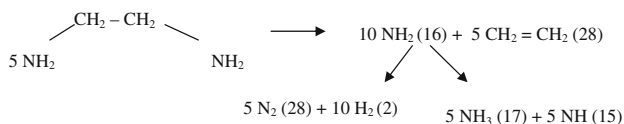
Stages	TG results			Percentage mass loss				Residue
	T_i/°C	T_f/°C	T_s/°C	Stepwise		Cumulative		
				Theoretical	Observed	Theoretical	Observed	
1	70	135	80	9.9	10.0	9.9	10.0	Ni(en)$_3$ C$_2$O$_4$
2	260	325	290	33.1	32.9	43	42.9	Ni(en) C$_2$O$_4$
3	325	400	385	36.4	35.3	79.4	78.2	NiO
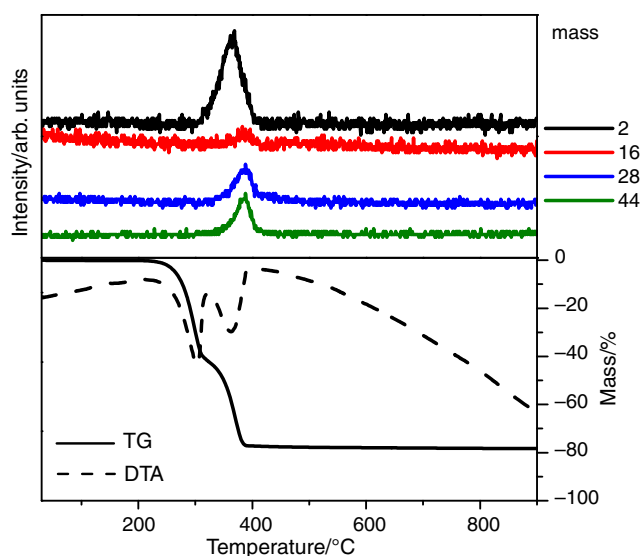
Fig. 2 TG/DTA-MS plot of tris(ethylenediamine)nickel(II) oxalate (in helium) at heating rate 10 °C min^{-1}

Fig. 3 XRD pattern of metallic nickel

molecules. The second stage begins at 320 °C and ends at 405 °C. The phenomenological data for the thermal decomposition of the dehydrated complex in helium is given in Table 3. The formation of metallic nickel as the final product is due to the reduction of NiO by CO formed during the decomposition [17]. The XRD pattern of the metallic nickel (JCPDS no. 04-0850) is shown in Fig. 3. Average crystallite size of metallic Ni calculated from the peak broadening value using Scherrer equation was found to be 22.5 nm.
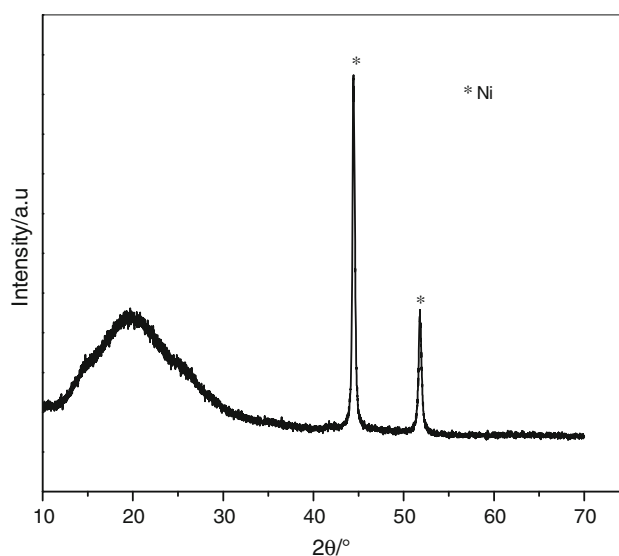
The DTA profile in Fig. 2 shows two endotherms with T_s values 298 and 370 °C corresponding to the two decomposition stages of tris(ethylenediamine)nickel(II) oxalate. The MS spectra of the complex show fragments with m/z values 2, 16, 28 and 44 in the temperature range 356–388 °C. The reported peaks are due to the evolution of H_2 (2), O/NH_2 (16), CO, N_2, $CH_2=CH_2$ (28) and CO_2 (44). The species H_2, NH_2, N_2 and $CH_2=CH_2$ are formed by the fragmentation of the evolved ethylenediamine as shown below.

Scheme 1 Fragmentation of ethylenediamine

Tris(ethylenediamine)nickel(II) sulphate

The thermal decomposition of tris(ethylenediamine)nickel(II) sulphate complex in air involves a four stage decomposition [18] as shown below:

$Ni(en)_3SO_4 \rightarrow Ni(en)SO_4 + 2en,$

$Ni(en)SO_4 \rightarrow NiSO_4 + en,$

$NiSO_4 \rightarrow$ mixture of NiO and $NiSO_4 \rightarrow NiO + SO_3.$

The phenomenological data for the thermal decomposition of tris(ethylenediamine)nickel(II) sulphate are given in Table 4. This complex starts to lose mass only at 300 °C, indicating the thermal stability of the complex. The stability is due to the strong coordination of the bidentate ligand (en) with nickel resulting in the formation of complex with octahedral geometry. The TG/DTA plot for the thermal decomposition of tris(ethylenediamine)nickel(II) sulphate in air at a heating rate of 10 °C min^{-1} is shown in Fig. 4. The first stage of decomposition of tris(ethylenediamine)nickel(II) sulphate corresponds to the loss of two molecules of ethylenediamine (36% loss) to give mono ethylenediamine complex. The mono(ethylenediamine)nickel(II) sulphate is very unstable and quickly decomposes at 360 °C. The subsequent stages are overlapping and hence not distinguishable. Intermediate

Table 3 Phenomenological data for the thermal decomposition of tris(ethylenediamine)nickel(II) oxalate in helium/$\phi = 10$ °C min^{-1}

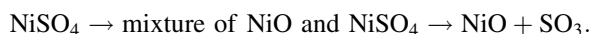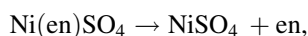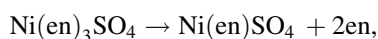| Stages	TG results			Percentage mass loss				Residue
	T_i/°C	T_f/°C	T_s/°C	Stepwise		Cumulative		
				Theoretical	Observed	Theoretical	Observed	
1	245	320	300	36.7	36.5	36.7	37.5	Ni(en)C$_2$O$_4$
2	320	405	375	45.3	42	82	78.5	Ni

Table 4 Phenomenological data for the thermal decomposition of tris(ethylenediamine)nickel(II) sulphate in air/$\phi = 10^\circ$C min^{-1}

| Stages	TG results			Percentage mass loss				Residue
	T_i/°C	T_f/°C	T_s/°C	Stepwise		Cumulative		
				Theoretical	Observed	Theoretical	Observed	
1	300	360	346	35.8	36	35.8	36	Ni(en) SO$_4$
2	360	466	424	17.9	17.9	53.7	53.9	NiSO$_4$
3	466	500	487					Mixture of NiSO$_4$ and NiO
4	696	786	760	23.9	23.9	77.6	77.8	NiO
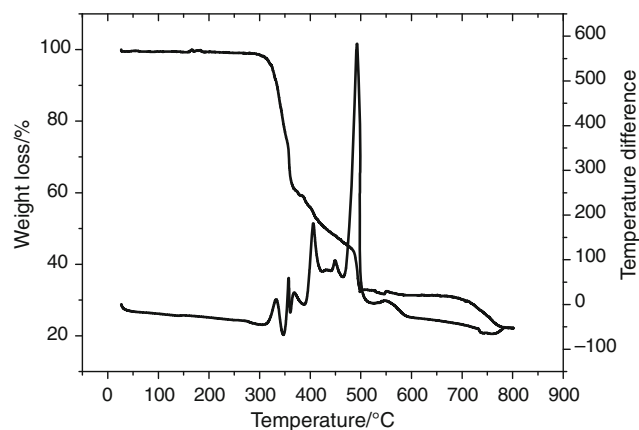
Fig. 4 TG/DTA plot of tris(ethylenediamine)nickel(II) sulphate (in air) at heating rate 10 °C min^{-1}
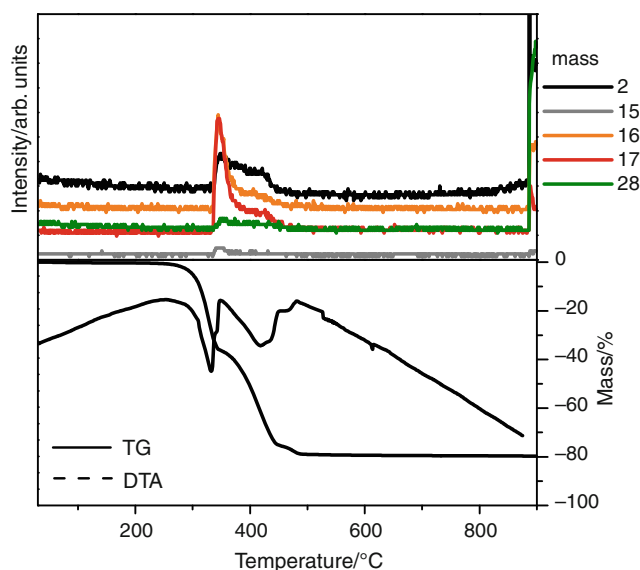
Fig. 5 TG/DTA-MS plot of tris(ethylenediamine)nickel(II) sulphate (in helium) at heating rate 10 °C min^{-1}

formed at 500 °C corresponds to the partial dissociation of NiSO$_4$ to a mixture of NiSO$_4$ and NiO phases. The total cumulative mass loss of 77.8% at 786 °C corresponds to the formation of NiO.

The plot of simultaneous TG/DTA coupled online with MS during the thermal decomposition of tris(ethylenediamine)nickel(II) sulphate in helium atmosphere is shown in Fig. 5. The TG–MS analysis indicates the following thermal decomposition patterns:
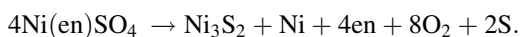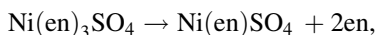
$$Ni(en)_3SO_4 \rightarrow Ni(en)SO_4 + 2en,$$

$$4Ni(en)SO_4 \rightarrow Ni_3S_2 + Ni + 4en + 8O_2 + 2S.$$

Tris(ethylenediamine)nickel(II) sulphate undergoes a two stage decomposition in helium atmosphere, resulting in the formation of a mixture of Ni and Ni$_3$S$_2$ (JCPDS no. 44-1418) phases as the residues. Figure 6 shows the XRD pattern of the decomposition products namely, Ni and Ni$_3$S$_2$. The mass spectra of tris(ethylenediamine)nickel(II) sulphate show peaks with m/z values 2, 15, 16, 17 and 28. These peaks are due to the presence of H$_2$, NH, NH$_2$, NH$_3$ and N$_2$/CH$_2$=CH$_2$. These species are formed due to the fragmentation of the liberated ethylenediamine molecule as shown in Scheme 1.
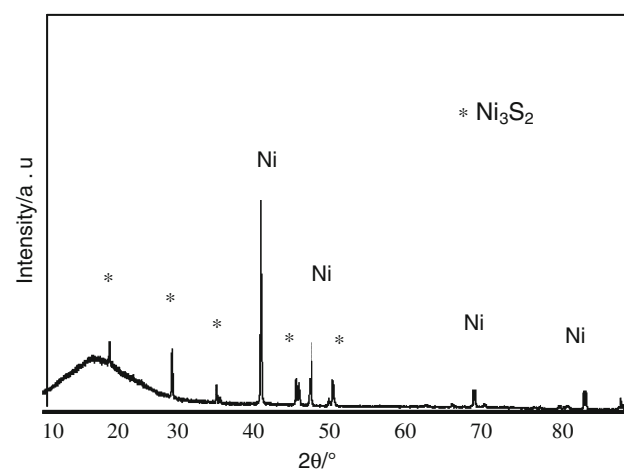
Fig. 6 XRD pattern of mixture Ni and Ni$_3$S$_2$

TR–XRD studies of the complexes

The high temperature XRD patterns of tris(ethylenediamine)nickel(II) oxalate dihydrate complex in the
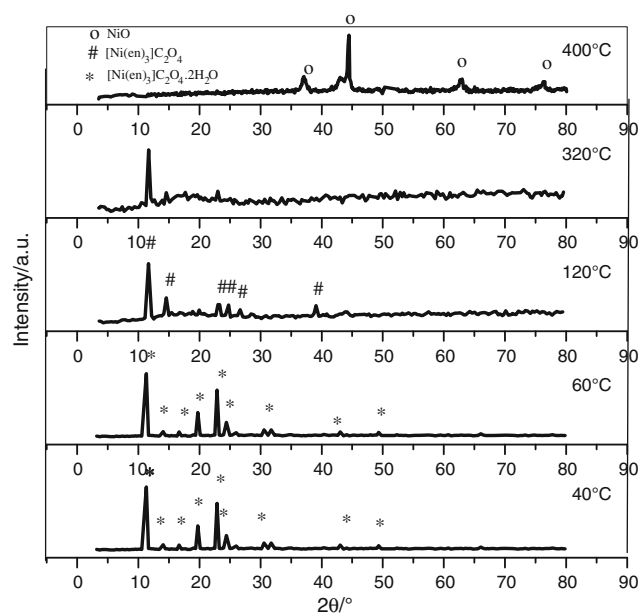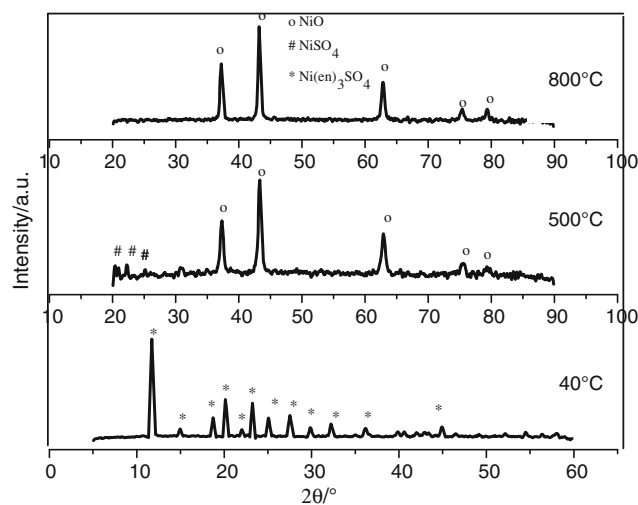
Fig. 7 High temperature XRD patterns of tris(ethylenediamine)nickel(II) oxalate dihydrate

temperature range 40–400 °C are shown in Fig. 7. The patterns recorded at 40–60 °C with peaks having 2θ values 11.29, 14.20, 16.60, 19.82, 22.98, 24.33, 30.80, 43.19 and 49.25 represent the planes of tris(ethylenediamine)nickel(II) oxalate dihydrate. Above 60 °C, the complex begins to decompose by the liberation of two molecules of water. The XRD pattern at 120 °C corresponds to the dehydrated complex. This complex is stable up to 240 °C and subsequently decomposes at 260 °C by releasing two en molecules. The XRD pattern at 320 °C corresponds to the monoethylenediamine complex. The monoethylenediamine complex decomposes at 400 °C to give NiO as the residue.

All the XRD patterns are highly crystalline and the final NiO residue formed contains well-defined peaks with fcc structure (JCPDS no. 47-1049). Average crystallite size of NiO was calculated from the peak broadening value using Scherrer equation and was found to be 23.4 nm.

The XRD patterns of tris(ethylenediamine)nickel(II) sulphate, intermediate and the residue are given in Fig. 8. The XRD pattern at 40 °C contains peaks corresponding to (100), (101), (002), (110), (102), (200), (201), (112), (202), (211), (301) and (303) planes of tris(ethylenediamine) nickel(II) sulphate (JCPDS no. 23-1796). The XRD pattern of the intermediate at 500 °C has peaks of $NiSO_4$ and NiO. However, the majority peaks are those of NiO phase. The XRD analysis revealed that the final residue at 800 °C is NiO and has well-defined peaks with cubic symmetry. From the peak broadening value, the crystallite size of NiO was calculated using Scherrer equation. Average crystallite size was found to be 17.47 nm.

Fig. 8 High temperature XRD patterns of tris(ethylenediamine) nickel(II) sulphate

SEM analyses

SEM images of tris(ethylenediamine)nickel(II) oxalate dihydrate, intermediates isolated at different temperatures and the residue in air are shown in Fig. 9. It is seen from SEM images that the complex has an elongated morphology. The SEM image shows that the dehydrated amine complex is having more or less same morphology as that of the original complex $[Ni(en)_3]C_2O_4.2H_2O$. This is due to the structural similarity of the complexes. Both these complexes possess octahedral geometry (as there is no change in coordination during the dehydration process) hence they exhibit similar structure. SEM image reveals that in the case of mono(ethylenediamine) nickel(II) oxalate there is an apparent change in morphology and a reduction of the size. The final residue NiO appears as very small rods.

The SEM pictures of tris(ethylenediamine)nickel(II) sulphate and the residue show that the complex has a rod like appearance and NiO (residue) is found to be agglomerated (Fig. 10).

Kinetic analyses

Kinetic analyses of the thermal decomposition of amine complexes were carried out by means of isoconversional methods. Isoconversional methods help to evaluate Arrhenius parameters without the prediction of a reaction model. The method yields a series of activation energies (E) as a function of conversion. Often the solid samples are polycrystalline in nature and hence the rates of solid state reactions are different for crystals of different size and occur in multi steps [19]. The effective activation energy of the process is a composite value determined by the

Fig. 9 SEM pictures of
a [Ni(en)$_3$]C$_2$O$_4$.2H$_2$O,
b [Ni(en)$_3$]C$_2$O$_4$, **c** Ni(en)C$_2$O$_4$,
d NiO
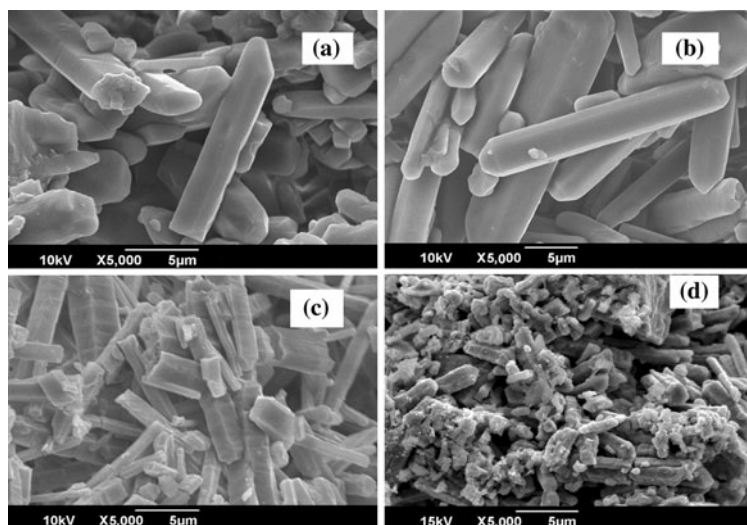
**Fig. 10** SEM pictures of
a [Ni(en)$_3$]SO$_4$, **b** NiO
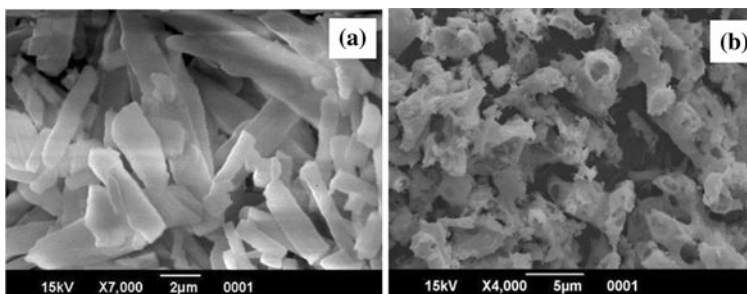
activation energies of elementary steps as well as by the relative contributions of these steps to the over all reaction rate. The contributions of the individual steps can change with the extent of conversion (α) and with the temperature (T). Hence, the variation of E with α is an indication of multi step kinetics [16]. From the dependence of activation energy on the extent of conversion, we can predict the nature of solid state reactions.

The activation energy versus conversion plot of tris(ethylenediamine)nickel(II) oxalate dihydrate for all three stages viz., dehydration, deamination and the decomposition are shown in Figs. 11a–c. It is observed that for the dehydration reaction (Fig. 11a), the activation energy decreases with conversion. The decreasing dependence shows that the reaction is reversible, which is very common to many solid state reactions of the type solid $\leftrightarrow$ solid + gas. This type of behaviour is a typical characteristic of the reversible dehydration of crystal hydrates like calcium oxalate monohydrate as well as other process showing reversible reactions [20]. For the deamination stage (stage II, Fig. 11b) also the activation energy decreases with conversion. This behaviour indicates that the deamination is a reversible reaction. For the final stage of decomposition (Fig. 11c), the activation energy derived from FWO and KAS equations decreases in the alpha range

0.05–0.2 and then increases ($\alpha = 0.4$). Increasing dependence of E on α shows that the reaction is competing or consecutive. Solid state reaction of the type solid $\rightarrow$ solid + gas, undergo such type of reactions. The activation energy (E) again decreases in the α range 0.45 to 1. Decreasing dependence shows the reaction is reversible in nature [20]. These variations of E with α, may be due to the occurrence of simultaneous deamination (loss of en) and decomposition (decomposition of nickel oxalate to give NiO, CO$_2$ and CO) steps in a single stage.

The kinetic analyses for the first deamination stage (i.e. Ni(en)$_3$SO$_4$ $\rightarrow$ Ni(en)SO$_4$ + 2 en) of tris(ethylenediamine)nickel(II) sulphate was derived using isoconversional methods and the corresponding kinetic plots are shown in Fig. 12. It is seen that the activation energy depends on conversion function (α) which indicates the complex decomposition mechanism. From the activation energy versus conversion plot using FWO and KAS equations, it is seen that activation energy was found to be decreasing with the extent of conversion in the range 0.05–0.7 and then found to be increasing [17]. As mentioned above, the decreasing dependence can be attributed to the reversible reactions and the increasing dependence can be attributed to the competing or consecutive reactions.

Fig. 11 Variation of activation
energy with conversion (α) for
a dehydration, **b** deamination,
c decomposition reactions of
tris(ethylenediamine)nickel(II)
oxalate dihydrate
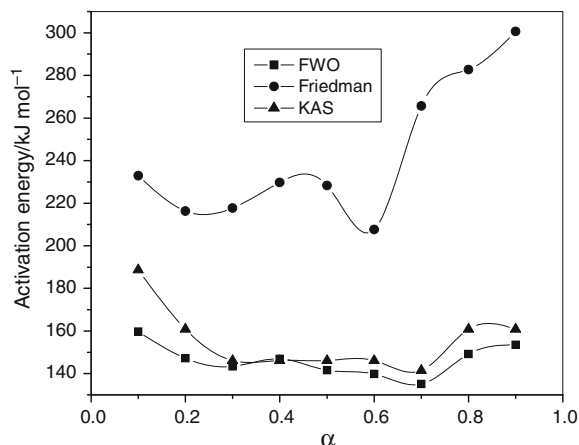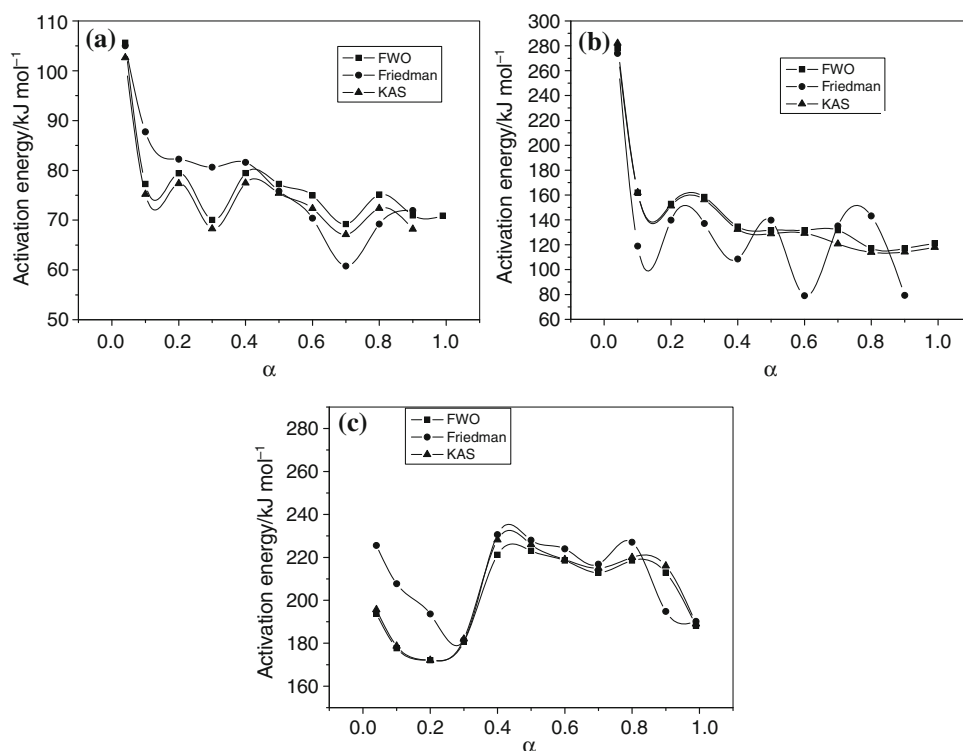
Fig. 12 Variation of activation energy with conversion (α) for the
deamination of [Ni(en)$_3$]SO$_4$ to Ni(en)SO$_4$

It is seen that the activation energy calculated by FWO
and KAS methods are comparable. However, the activation
energies calculated by Friedman method show higher values
in most cases. This is because the Friedman method is very
sensitive to experimental noise and tends to be numerically
unsound when employing instantaneous rate values [21].

Conclusions

Thermal behaviour of [Ni(en)$_3$]C$_2$O$_4$·2H$_2$O and [Ni(en)$_3$]
SO$_4$ have been carried out in different atmospheric

conditions (air and He). In air, tris(ethylenedia-
mine)nickel(II) oxalate dihydrate decomposes in three
steps and tris(ethylenediamine)nickel(II) sulphate decom-
poses in four steps. In air, both the complexes give nickel
oxide as the final product of decomposition. In helium
atmosphere, the dehydrated tris(ethylenediamine)nickel(II)
oxalate complex undergoes a two step decomposition to
give nickel as the final product. Tris(ethylenedia-
mine)nickel(II) sulphate undergoes a two stage decompo-
sition in helium and gives a mixture of nickel and nickel
sulphide as the final residues. Simultaneous TG/DTA
coupled online with mass spectra (MS) in helium atmo-
sphere revealed the presence of H$_2$, O, CO, N$_2$ and CO$_2$
fragments during the decomposition of tris(ethylenedia-
mine)nickel(II) oxalate and H$_2$, O, NH, NH$_2$, NH$_3$ and N$_2$ in
the case of tris(ethylenediamine)nickel(II) sulphate decom-
position. SEM analyses show that both tris(ethylenedia-
mine)nickel(II) oxalate dihydrate and tris(ethylenediamine)
nickel(II) sulphate complexes have rod like appearances.
Kinetic analyses by isoconversional methods reveal that the
dehydration and deamination stages of tris(ethylenedia-
mine)nickel(II) oxalate dihydrate are reversible in nature.
The decomposition reaction of the tris(ethylenediamine)
nickel(II) oxalate dihydrate and the first deamination stage of
tris(ethylenediamine)nickel(II) sulphate show increasing as
well as decreasing dependence of activation energy on
conversion, probably due to the simultaneous occurrence of
various thermal events in a single stage.

References

1. Singh G, Pandey DK. Studies on energetic compounds: kinetics and mechanism of thermolysis of bis(ethylenediamine)metal nitrate and their role in the burning rate of solid propellants. Propellants Explos Pyrotech. 2003;28:231–9.
2. Mathew S, Nair CGR, Ninan KN. Thermal decomposition studies on amine complexes of copper(II) nitrate in solid state. Bull Chem Soc Jpn. 1991;64:3207–9.
3. Mathew S, Nair CGR, Ninan KN. Kinetics and mechanism of thermal decomposition of bis(ethylenediamine)copper(II) halide monohydrate. Thermochim Acta. 1991;181:253–68.
4. Ozawa T. A new method of analyzing thermogravimetric data. Bull Chem Soc Jpn. 1965;38:1881–6.
5. Flynn JH, Wall LA. A quick, direct method for the determination of activation energy from thermogravimetric data. J Polym Sci B. 1996;4:323–8.
6. Friedman HL. New methods for evaluating kinetic parameters from thermal analysis data. J Polym Sci B. 1969;7:41–6.
7. Kissinger HE. Reaction kinetics in differential thermal analysis. Anal Chem. 1957;29:1702–6.
8. Akahira T, Sunose T. Research report of Chiba Institute Technology. Sci Technol. 1971;16:22–31.
9. Haschke JM, Wendlandt WW. The thermal decomposition of metal ethylenediamine complexes. Anal Chim Acta. 1965;32:386–93.
10. Rochow EG, editor. Inorganic synthesis, vol VI. New York: McGraw-Hill; 1960. p. 198–200.
11. Vogel AG. Text book of quantitative inorganic analysis. 4th ed. Longmann: London; 1978.
12. Cai JM, Bi LS. Kinetic analysis of wheat straw pyrolysis using isoconversional methods. J Therm Anal Calorim. 2009;98:325–30.
13. Su TT, Zhai YC, Jiang H, Gong H. Studies on the thermal decomposition kinetics and mechanism of ammonium niobium oxalate. J Therm Anal Calorim. 2009;98:449–55.
14. Badrinarayanan P, Zheng W, Simon SL. Isoconversional analysis of the glass transition. Thermochim Acta. 2008;468:87–93.
15. Jankovic B, Adnadevic B, Javanovic J. Application of model fitting and model free kinetics to the study of non isothermal dehydration of equilibrium swollen poly(acrylic acid) hydrogel: thermogravimetric analysis. Thermochim Acta. 2007;452:106–15.
16. Vyazovkin S. A unified approach to kinetic processing of non-isothermal data. Int J Chem Kinet. 1996;28:95–101.
17. Małecka B, Małecki A, Drożdż-Cieśla E, Tortet L, Llewellyn P, Rouquerol F. Some aspects of thermal decomposition of $NiC_2O_4 \cdot 2H_2O$. Thermochim Acta. 2007;466:57–62.
18. Rejitha KS, Mathew S. Thermal deamination kinetics of tris(ethylenediamine)nickel(II) sulphate in the solid state. J Therm Anal Calorim. 2008;93:213–7.
19. Vyazovkin S. Kinetic concepts of thermally stimulated reactions in solids: a view from a historical perspective. Int Rev Phys Chem. 2000;19:45–60.
20. Vyazovkin S, Linert W. Kinetic analysis of reversible thermal decomposition of solids. Int J Chem Kinet. 1995;27:73–84.
21. Vyazovkin S. Modification of the integral isoconversional method to account for variation in the activation energy. J Comput Chem. 2001;22:178–83.